A Novel Analog Signal Transmission using Joint Space-Time Transmit Diversity and Receive Antenna Diversity

Thanh Hai VO † Shinya KUMAGAI † and Fumiyuki ADACHI ‡
Dept. of Communications Engineering, Graduate School of Engineering, Tohoku University
6-6-05 Aza-Aoba, Aramaki, Aoba-ku, Sendai, Miyagi, 980-8579 Japan
† {vothanhhai, kumagai}@mobile.ecei.tohoku.ac.jp, ‡ adachi@ecei.tohoku.ac.jp

***Abstract*—Recently, we proposed a novel analog signal transmission technique called analog single-carrier transmission with frequency-domain equalization (analog SC-FDE) and showed that analog SC-FDE achieves better normalized mean square error (NMSE) performance than conventional analog signal transmission. In order to achieve further performance improvement, transmit/receive antenna diversity technique is effective. In digital wireless communications, joint space-time transmit diversity (STTD) and receive antenna diversity is well known as a promising antenna diversity technique which achieves a high diversity order (equal to the product of the number of transmit antennas and the number of receive antennas) with a simple signal processing. In this paper, analog SC-FDE using joint STTD and receive antenna diversity is proposed. A theoretical analysis of the NMSE performance is derived to evaluate the transmission performance of the proposed scheme and is confirmed by computer simulation. We show that joint STTD and receive antenna diversity can significantly improve the NMSE performance of our proposed analog SC-FDE.**

Keywords—analog signal transmission; frequency-domain equalization; single-carrier transmission; space-time transmit diversity; receive antenna diversity

I. INTRODUCTION

Nowadays, although digital signal transmission has been continuously evolving [1]-[2], analog signal transmission (e.g., radio broadcasting) still remains essential. In comparison with the digital signal transmission, the signal bandwidth of analog signal transmission is much narrower since neither source coding nor channel coding is required. However, the channel in analog signal transmission is a frequency-nonselective fading channel [2]. As a consequence of suffering from the frequency-nonselective fading channel, the received signal power drops over a consecutive period of time and hence, the received signal quality significantly degrades. In order to overcome this problem, we recently proposed a novel analog signal transmission technique that is referred to as analog single-carrier transmission using frequency-domain equalization (analog SC-FDE) [3]. Analog SC-FDE applies discrete Fourier transform (DFT), frequency-domain spectrum shaping and mapping, inverse DFT (IDFT), and cyclic prefix (CP) insertion before transmission. At the receiver, one-tap frequency-domain equalization (FDE) [4] is applied to take advantage of frequency-selective fading channel. Normalized mean square error (NMSE) performance was used to evaluate the proposed analog SC-FDE and we showed that it achieves better NMSE performance than conventional analog signal transmission. In particular, combining distributed mapping and minimum mean square error (MMSE) equalization gives the best performance [3].

In order to further improve the transmission performance, transmit/receive antenna diversity is a well-known effective technique [5]. For digital signal transmission, space-time transmit diversity (STTD) [6] has recently drawn great attention as a promising diversity technique. Furthermore, joint STTD and receive antenna diversity [7] can achieve the maximum ratio combining (MRC) diversity with order of the product of the number of transmit antennas and the number of receive antennas [8]. At the receiver, STBC decoding can be performed in conjunction with MMSE equalization to improve the transmission performance. In this paper, analog SC-FDE using joint STTD and receive antenna diversity is proposed in order to further improve the transmission performance. A theoretical analysis of NMSE performance is presented and confirmed by computer simulation to evaluate analog SC-FDE using joint STTD and receive antenna diversity.

The remainder of this paper is organized as follows. In Section II, analog SC-FDE using joint STTD and receive antenna diversity is presented. Theoretical analysis of NMSE performance is given in Section III. Section IV provides the numerical evaluation and computer simulation results. Finally, conclusion is presented in Section V.

II. ANALOG SC-FDE USING JOINT SPACE-TIME TRANSMIT DIVERSITY AND RECEIVE ANTENNA DIVERSITY

A. System Model

System model of analog SC-FDE using joint STTD and receive antenna diversity is illustrated in Fig. 1. At the transmitter having N_t transmit antennas, after the signal bandwidth is limited by low-pass filter (LPF), the analog signal $s(t)$ to be transmitted is sampled at the Nyquist rate. Then, the sample sequence is grouped into a sequence of signal blocks of M samples each. Each signal block $\{s(n);\ n=0\sim M-1\}$ is transformed by M-point DFT into frequency-domain signal block. Spectrum shaping filter is introduced in order to generalize the proposed system model having a specific spectrum shaping design. Next, STBC encoding is implemented to obtain N_t parallel streams of encoded signal blocks. The resultant M frequency components, which are referred to as M subcarriers, of each encoded block are mapped over a broad bandwidth having N_c ($>M$) orthogonal subcarriers with zeros occupying the unused subcarriers. Then, each encoded block of N_c subcarriers is transformed back into complex time-domain signal block $\{x_{q,n_t}(n);\ n=0\sim N_c-1\}$ by N_c-point IDFT. Finally, the last N_g samples of each transmission block are copied as a CP and inserted into the guard interval placed at the beginning of each transmit block.

The CP-inserted signal blocks are transmitted from N_t antennas over a frequency-selective fading channel. N_r receive antennas are used at the receiver. After removing CP, each

978-1-4799-4449-1/14/$31.00 ©2014 IEEE

block is transformed into the frequency-domain signal block by N_c-point DFT. De-mapping is then performed to pick up desired M subcarriers before joint STBC decoding and one-tap MMSE-FDE is applied to demodulate M-subcarrier blocks of original signal. Next, each M-subcarrier block is transformed back into complex time-domain signal. Real part of the signal is outputted and finally, the analog signal $\tilde{s}(t)$ is reconstructed by automatic gain control (AGC) [9] and LPF.

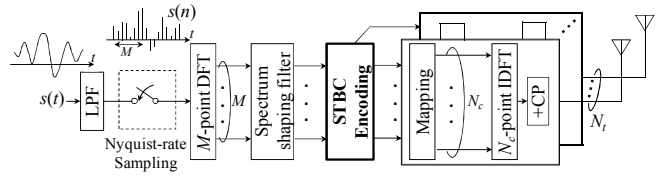

(a) Transmitter

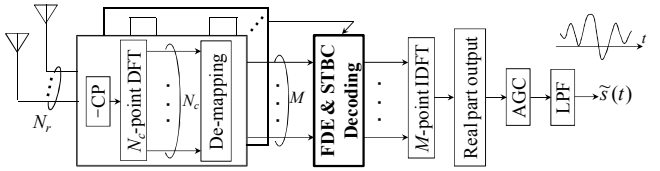

(b) Receiver

Fig. 1. System model.

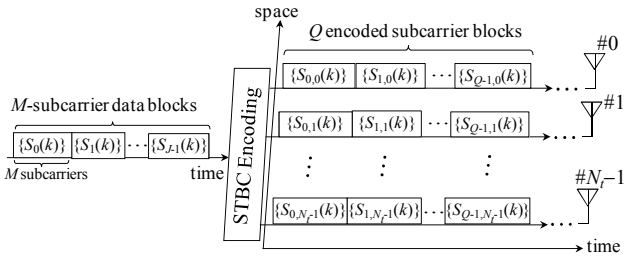

Fig. 2. STBC encoding.

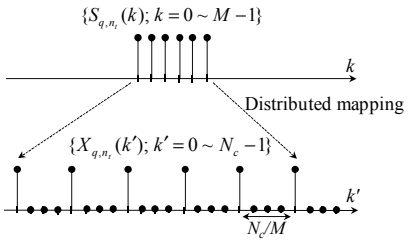

Fig. 3. Subcarrier mapping.

TABLE I. RELATIONSHIP OF N_T, J, Q, AND CODING RATE R_{STBC}

N_t	J	Q	$R_{STBC}=J/Q$
1	1	1	1
2	2	2	1
3	3	4	3/4
4	3	4	3/4

B. STBC Encoding for Analog SC-FDE

At the transmitter, we assume that spectrum shaping filter is an ideal brick wall LPF. After applying DFT and spectrum shaping filter, J blocks of M subcarriers are grouped $\{S_j(k); k=0\sim M-1, j=0\sim J-1\}$ and expressed as

$$S_j(k)=\frac{1}{\sqrt{M}}\sum_{n=0}^{M-1}s_j(n)\exp\left(-j2\pi k\frac{n}{M}\right). \quad (1)$$

Then, the grouped J blocks are encoded by STBC encoding into N_t parallel streams of Q encoded subcarrier blocks $\{S_{q,n_t}(k);\ k=0\sim M-1,\ q=0\sim Q-1,\ n_t=0\sim N_t-1\}$ as shown in Fig. 2. The numbers of subcarrier blocks J and Q depended on the number of transmit antennas N_t are shown in Table I for $N_t=1\sim4$. The coding rate $R_{STBC}=J/Q$ decreases when N_t increases. N_t parallel streams of Q encoded subcarrier blocks are represented as $N_t\times Q$ space-time encoding matrix $\mathbf{S}_{N_t}=[\mathbf{S}_0(k),...,\mathbf{S}_q(k),...,\mathbf{S}_{Q-1}(k)]$, where $\mathbf{S}_q(k)=[S_{q,0}(k),...,S_{q,n_t}(k),...,S_{q,N_t-1}(k)]^T$ is the q-th encoded frequency-domain signal vector at the k-th frequency [8] and $[.]^T$ denotes the transpose operation.

$$\mathbf{S}_{N_t=1}(k)=S_0(k), \quad (2.a)$$

$$\mathbf{S}_{N_t=2}(k)=\frac{1}{\sqrt{2}}\begin{bmatrix}S_0(k) & -S_1^*(k)\\ S_1(k) & S_0^*(k)\end{bmatrix}, \quad (2.b)$$

$$\mathbf{S}_{N_t=3}(k)=\frac{1}{\sqrt{3}}\begin{bmatrix}S_0(k) & -S_1^*(k) & -S_2^*(k) & 0\\ S_1(k) & S_0^*(k) & 0 & -S_2^*(k)\\ S_2(k) & 0 & S_0^*(k) & S_1^*(k)\end{bmatrix}, \quad (2.c)$$

$$\mathbf{S}_{N_t=4}(k)=\frac{1}{\sqrt{4}}\begin{bmatrix}S_0(k) & -S_1^*(k) & -S_2^*(k) & 0\\ S_1(k) & S_0^*(k) & 0 & -S_2^*(k)\\ S_2(k) & 0 & S_0^*(k) & S_1^*(k)\\ 0 & S_2(k) & -S_1(k) & S_0(k)\end{bmatrix}, \quad (2.d)$$

in which $[.]^*$ denotes the complex conjugate operation.

For each encoded block, distributed mapping [10] is considered in order to enhance frequency diversity gain obtained at the receiver [3]. M subcarriers of each encoded block $\{S_{q,n_t}(k);\ k=0\sim M-1\}$ are mapped equally over a broad bandwidth having N_c ($>M$) orthogonal subcarriers expressed as $\{X_{q,n_t}(k');\ k'=0\sim N_c-1\}$ in Eq. (3) in which zero occupies the unused subcarriers. An example of subcarrier mapping with $M=6$, $N_c=24$ is illustrated in Fig. 3.

$$X_{q,n_t}(k')=\begin{cases}S_{q,n_t}(k) & ,\ k'=k\times\dfrac{N_c}{M}\\ 0 & ,\ otherwise\end{cases}, \quad (3)$$

where $k=0\sim M-1$, $k'=0\sim N_c-1$, $q=0\sim Q-1$, $n_t=0\sim N_t-1$ and N_c/M is the adjacent subcarrier interval. After N_c-point IDFT, the time-domain sample sequence at a rate of $1/T_s=(N_c/M)\times1/T$, in which $1/T$ is the Nyquist sampling rate of analog signal $s(t)$, is obtained. The CP-inserted time-domain sample sequence $\{\tilde{x}_{q,n_t}(n);\ n=-N_g\sim N_c-1\}$ can be expressed using the equivalent low-pass representation as

$$\tilde{x}_{q,n_t}(n)=\sqrt{2P}\,x_{q,n_t}(n \bmod N_c), \quad (4)$$

in which P is the average sample sequence power and $\{x_{q,n_t}(n);\ n=0\sim N_c-1\}$ is given by

$$x_{q,n_t}(n)=\frac{1}{\sqrt{N_c}}\sum_{k=0}^{N_c-1}X_{q,n_t}(k)\exp\left(j2\pi\frac{k}{N_c}n\right). \quad (5)$$

C. Received Signal

Assuming that the channel consists of L distinct propagation paths, the channel impulse response $h_{n_r,n_t}(\tau)$ can be expressed as

$$h_{n_r,n_t}(\tau)=\sum_{l=0}^{L-1}h_{n_r,n_t,l}\delta(\tau-\tau_{n_r,n_t,l}), \quad (6)$$

where $h_{n_r,n_t,l}$, $\tau_{n_r,n_t,l}$, and $\delta(.)$ are complex-valued path gain with $E[\sum_{l=0}^{L-1}|h_{n_r,n_t,l}|^2]=1$ ($E[.]$ denotes ensemble average operation), symbol-spaced time delay of the l-th path (i.e.,

$\tau_{n_r,n_t,l} = l$), and delta function, respectively. In Eq. (6), we assume that the channel stays constant during the signal transmission period of Q encoded blocks. It is assumed that the maximum time delay of channel is shorter than CP and the received signal is ideally sampled at the rate $1/T_s$.

At the receiver, the superposition of N_t transmitted signals is received by N_r receive antennas. The discrete-time received signal $\{r_{q,n_r}(t);\ t=-N_g\sim N_c-1,\ q=0\sim Q-1,\ n_r=0\sim N_r-1\}$ at n_r-th receive antenna is expressed as

$$r_{q,n_r}(t) = \sum_{n_t=0}^{N_t-1}\sum_{l=0}^{L-1} h_{n_r,n_t,l}\,\tilde{x}_{q,n_t}(t-\tau_{n_r,n_t,l}) + n_{q,n_r}(t), \qquad (7)$$

where $n_{q,n_r}(t)$ is the additive white Gaussian noise (AWGN) with zero-mean and variance $2N_0/T_s$ in which N_0 is the single-sided power spectrum density. After removing CP, the receiver transforms each received signal block into the frequency-domain signal using N_c-point DFT. The frequency-domain received signal at the k-th frequency $\{R_{q,n_r}(k);\ k=0\sim N_c-1,\ q=0\sim Q-1,\ n_r=0\sim N_r-1\}$ is expressed as

$$R_{q,n_r}(k) = \sqrt{2P}\sum_{n_t=0}^{N_t-1} H_{n_r,n_t}(k)X_{q,n_t}(k) + \prod_{q,n_r}(k), \qquad (8)$$

where $H_{n_r,n_t}(k)$ and $\prod_{q,n_r}(k)$ are respectively the channel gain and the noise component at the k-th frequency given by

$$H_{n_r,n_t}(k) = \sum_{l=0}^{L-1} h_{n_r,n_t,l}\exp\left(-j2\pi k\frac{\tau_{n_r,n_t,l}}{N_c}\right), \qquad (9)$$

$$\prod_{q,n_r}(k) = \frac{1}{\sqrt{N_c}}\sum_{t=0}^{N_c-1} n_{q,n_r}(t)\exp\left(-j2\pi k\frac{t}{N_c}\right). \qquad (10)$$

De-mapping is then performed to obtain desired M frequency components $\{\hat{R}_{q,n_r}(k);\ k=0\sim M-1,\ q=0\sim Q-1,\ n_r=0\sim N_r-1\}$ of original signal. Channel gain $\{\hat{H}_{n_r,n_t}(k);\ k=0\sim M-1,\ n_t=0\sim N_t-1,\ n_r=0\sim N_r-1\}$ for FDE and the equivalent noise component $\{\hat{\prod}_{q,n_t}(k);\ k=0\sim M-1,\ q=0\sim Q-1,\ n_r=0\sim N_r-1\}$ are also obtained as

$$\begin{cases}\hat{R}_{q,n_r}(k) = R_{q,n_r}(k\times N_c/M)\\ \hat{H}_{n_r,n_t}(k) = H_{n_r,n_t}(k\times N_c/M)\\ \hat{\prod}_{q,n_r}(k) = \prod_{q,n_r}(k\times N_c/M)\end{cases}. \qquad (11)$$

D. Joint STBC Decoding and MMSE-FDE

After the subcarrier de-mapping, one-tap MMSE-FDE is carried out as

$$[\tilde{\mathbf{R}}_0(k),...,\tilde{\mathbf{R}}_{Q-1}(k)] = \mathbf{W}^H(k)[\hat{\mathbf{R}}_0(k),...,\hat{\mathbf{R}}_{Q-1}(k)], \qquad (12)$$

where $\tilde{\mathbf{R}}_q(k) = [\tilde{R}_{q,0}(k),...,\tilde{R}_{q,n_r-1},...,\tilde{R}_{q,N_r-1}(k)]^T$ and $\hat{\mathbf{R}}_q(k) = [\hat{R}_{q,0}(k),...,\hat{R}_{q,n_r-1}(k),...,\hat{R}_{q,N_r-1}(k)]^T$ for $q=0\sim Q-1$ with $[.]^H$ denotes the Hermitian transpose operation. $\mathbf{W}(k) = [\mathbf{W}_0(k),...,\mathbf{W}_{n_r}(k),...,\mathbf{W}_{N_r-1}(k)]$ in which $\mathbf{W}_{n_r}(k) = [W_{n_r,0}(k),...,W_{n_r,n_t}(k),...,W_{n_r,N_t-1}(k)]^T$ is an $N_r \times N_t$ MMSE-FDE weight matrix with $W_{n_r,n_t}(k)$ being given by [8]

$$W_{n_r,n_t}(k) = \frac{\hat{H}_{n_r,n_t}(k)}{\frac{1}{N_t}\sum_{n_r=0}^{N_r-1}\sum_{n_t=0}^{N_t-1}\left|\hat{H}_{n_r,n_t}(k)\right|^2 + \Gamma^{-1}}. \qquad (13)$$

In Eq. (13), $k=0\sim M-1$ and $\Gamma = PT_s/N_0$ is the average received signal-to-noise power ratio (SNR).

Next, STBC decoding is applied to demodulate M-subcarrier blocks of original signal as shown below. The k-th subcarrier group is expressed as demodulated subcarrier vector $\tilde{\mathbf{S}}_{N_t}(k) = [\tilde{S}_0(k),...,\tilde{S}_{J-1}(k)]^T$ for $k=0\sim M-1$.

$$\tilde{\mathbf{S}}_{N_t=1}(k) = \tilde{R}_{0,0}(k), \qquad (14.a)$$

$$\tilde{\mathbf{S}}_{N_t=2}(k) = \begin{bmatrix}\tilde{R}_{0,0}(k)+\tilde{R}^*_{1,1}(k)\\ \tilde{R}_{0,1}(k)-\tilde{R}^*_{1,0}(k)\end{bmatrix}, \qquad (14.b)$$

$$\tilde{\mathbf{S}}_{N_t=3}(k) = \begin{bmatrix}\tilde{R}_{0,0}(k)+\tilde{R}^*_{1,1}(k)+\tilde{R}^*_{2,2}(k)\\ \tilde{R}_{0,1}(k)-\tilde{R}^*_{1,0}(k)+\tilde{R}^*_{3,2}(k)\\ \tilde{R}_{0,2}(k)-\tilde{R}^*_{2,0}(k)-\tilde{R}^*_{3,1}(k)\end{bmatrix}, \qquad (14.c)$$

$$\tilde{\mathbf{S}}_{N_t=4}(k) = \begin{bmatrix}\tilde{R}_{0,0}(k)+\tilde{R}^*_{1,1}(k)+\tilde{R}^*_{2,2}(k)+\tilde{R}_{3,3}(k)\\ \tilde{R}_{0,1}(k)-\tilde{R}^*_{1,0}(k)-\tilde{R}_{2,3}(k)+\tilde{R}^*_{3,2}(k)\\ \tilde{R}_{0,2}(k)+\tilde{R}_{1,3}(k)-\tilde{R}^*_{2,0}(k)-\tilde{R}^*_{3,1}(k)\end{bmatrix}. \qquad (14.d)$$

After transforming the frequency-domain signal $\{\tilde{S}_j(k);\ k=0\sim M-1,\ j=0\sim J-1\}$ back into the time-domain signal by M-point IDFT and applying AGC, only the real part of the time-domain signal $\{\tilde{s}_j(n);\ n=0\sim M-1,\ j=0\sim J-1\}$ is outputted as

$$\tilde{s}_j(n) = s_j(n) + \mathrm{Re}\{\mu_{\mathrm{ISI}}(n) + \mu_{\mathrm{noise}}(n)\}, \qquad (15)$$

where $\mu_{\mathrm{ISI}}(n)$ and $\mu_{\mathrm{noise}}(n)$ are residual signal distortion, and equivalent noise, respectively.

III. Normalized Mean Square Error Analysis

In this paper, in order to evaluate transmission performance of analog SC-FDE using joint STTD and receive antenna diversity, we use NMSE criterion which is defined as

$$\mathrm{NMSE} \equiv \frac{E[|\tilde{s}(n)-s(n)|^2]}{E[|s(n)|^2]}. \qquad (16)$$

Without loss of generality, the transmit signal is assumed to have unit average power. Using Eq. (15), NMSE can be written as

$$\mathrm{NMSE} = E[|\mathrm{Re}\{\mu_{\mathrm{ISI}}(n)+\mu_{\mathrm{noise}}(n)\}|^2]. \qquad (17)$$

Since $\mu_{\mathrm{ISI}}(n)$ and $\mu_{\mathrm{noise}}(n)$ are statistically independent, the variance of $\mu(n) = \mu_{\mathrm{ISI}}(n)+\mu_{\mathrm{noise}}(n)$ is expressed as

$$2\sigma^2_{\mu} = E[|\mu(n)|^2] = 2\sigma^2_{\mu_{\mathrm{ISI}}} + 2\sigma^2_{\mathrm{noise}}. \qquad (18)$$

By using some manipulations, $\sigma^2_{\mu_{\mathrm{ISI}}}$ and $\sigma^2_{\mathrm{noise}}$ are derived as (the derivation is shown in Appendix)

$$\begin{aligned}\sigma^2_{\mu_{\mathrm{ISI}}} &= E[|\mathrm{Re}\{\mu_{\mathrm{ISI}}(n)\}|^2] = \frac{1}{2}E[|\mu_{\mathrm{ISI}}(n)|^2]\\ &= \frac{1}{2}\left\{\frac{\frac{1}{M}\sum_{k=0}^{M-1}\left|\sum_{n_r=0}^{N_r-1}\sum_{n_t=0}^{N_t-1}\tilde{H}_{n_r,n_t}(k)\right|^2}{\left|\frac{1}{M}\sum_{k=0}^{M-1}\sum_{n_r=0}^{N_r-1}\sum_{n_t=0}^{N_t-1}\tilde{H}_{n_r,n_t}(k)\right|^2} - 1\right\},\end{aligned} \qquad (19)$$

$$\begin{aligned}\sigma^2_{\mu_{\mathrm{noise}}} &= E[|\mathrm{Re}\{\mu_{\mathrm{noise}}(n)\}|^2] = \frac{1}{2}E[|\mu_{\mathrm{noise}}(n)|^2]\\ &= \frac{1}{2}\times\frac{N_t\times\frac{1}{\Gamma}\times\frac{1}{M}\sum_{k=0}^{M-1}\sum_{n_r=0}^{N_r-1}\sum_{n_t=0}^{N_t-1}\left|W_{n_r,n_t}(k)\right|^2}{\left|\frac{1}{M}\sum_{k=0}^{M-1}\sum_{n_r=0}^{N_r-1}\sum_{n_t=0}^{N_t-1}\tilde{H}_{n_r,n_t}(k)\right|^2},\end{aligned} \qquad (20)$$

where $\tilde{H}_{n_r,n_t}(k) = W^*_{n_r,n_t}(k)\hat{H}_{n_r,n_t}(k)$ is the equivalent channel after MMSE-FDE. Therefore, the conditional NMSE for given set of channel gains $\{H_{n_r,n_t}(k);\ k=0\sim M-1,\ n_r=0\sim N_r-1,\ n_t=0\sim N_t-1\}$ can be obtained from Eqs. (17), (19), and (20) as

$$\mathrm{NMSE}\left(\Gamma,\{H_{n_r,n_t}(k)\}\right) = \frac{1}{2}\left\{\frac{\frac{1}{M}\sum_{k=0}^{M-1}\left|\sum_{n_r=0}^{N_r-1}\sum_{n_t=0}^{N_t-1}\tilde{H}_{n_r,n_t}(k)\right|^2}{\left|\frac{1}{M}\sum_{k=0}^{M-1}\sum_{n_r=0}^{N_r-1}\sum_{n_t=0}^{N_t-1}\tilde{H}_{n_r,n_t}(k)\right|^2}\right.$$

$$\left. + \frac{N_t\times\frac{1}{\Gamma}\times\frac{1}{M}\sum_{k=0}^{M-1}\sum_{n_r=0}^{N_r-1}\sum_{n_t=0}^{N_t-1}\left|W_{n_r,n_t}(k)\right|^2}{\left|\frac{1}{M}\sum_{k=0}^{M-1}\sum_{n_r=0}^{N_r-1}\sum_{n_t=0}^{N_t-1}\tilde{H}_{n_r,n_t}(k)\right|^2} - 1\right\}. \quad (21)$$

The theoretical average NMSE can be numerically evaluated by averaging Eq. (21) over $\{H_{n_r,n_t}(k);\ k=0\sim N_c-1,\ n_r=0\sim N_r-1,\ n_t=0\sim N_t-1\}$ as

$$\mathrm{NMSE}(\Gamma) = \int\ldots\int \mathrm{NMSE}\left(\Gamma,\{H_{n_r,n_t}(k)\}\right)\prod_{n_r,n_t,k} dH_{n_r,n_t}(k) \quad (22)$$

IV. Numerical Evaluation and Computer Simulation

A. Numerical Evaluation and Computer Simulation Condition

The condition for numerical evaluation of the theoretical average NMSE and the computer simulation is summarized in Table II. We assume the bandwidth-limited (4 kHz) voice transmission. A sampling rate of 8 kHz, a time-domain signal block with length of M = 64 samples, an adjacent subcarrier interval of 125 Hz, and a distributed subcarrier mapping over N_c = 8192 subcarriers are assumed. As a propagation channel, a frequency-selective block Rayleigh fading channel having an L=16-path uniform power delay profile is considered. The time delay of the l-th path is set to $\tau_{n_r,n_t,l} = l$ and the maximum delay difference is less than CP length (i.e., $L-1 \le N_g$). Ideal channel estimation and fast AGC are also assumed.

The numerical evaluation of the theoretical average NMSE is done by Monte-Carlo numerical computation method as follows. The set of path gains $\{h_{n_r,n_t,l};\ l=0\sim L-1\}$ is generated for obtaining $\{H_{n_r,n_t}(k);\ k=0\sim N_c-1\}$ and $\{W_{n_r,n_t}(k);\ k=0\sim M-1\}$ using Eqs. (9) and (13), respectively. The conditional NMSE for the given average SNR Γ is computed using Eq. (21). This is repeated sufficient times to obtain the average NMSE given by Eq. (22).

B. NMSE performance

The NMSE performance of the proposed analog SC-FDE using joint STTD and receive antenna diversity is shown in Fig. 4. A fairly good agreement between the simulation and theoretical results is seen. The NMSE performance is significantly improved when the number of transmit/receive antenna increases because of achieving higher antenna diversity gain. It is shown that analog SC-FDE using joint STTD and receive antenna diversity in case of (N_t,N_r) = (2,4) can reduce about 12 dB of the required SNR compared to analog SC-FDE (i.e., (N_t,N_r) = (1,1)) for achieving average NMSE = 10^{-2}. In case of increasing the number of transmit antennas, although higher antenna diversity gain is achievable, the NMSE performance improvement is small due to the decrease of transmit power per antenna (i.e., the increase of the equivalent noise power according to Eq. (20)).

TABLE II. Computer Simulation Condition

Signal transmission	Analog SC-FDE using joint STTD & Rx antenna diversity
Total no. of subcarriers	N_c=8192
Time-domain block length	M=64
No. of Tx antennas	N_t=1~4
No. of Rx antennas	N_r=1~4
Spectrum shaping filter	Ideal brick wall LPF
CP size	N_g=16
Sampling rate	$1/T$=8kHz
Mapping	Distributed
Channel	Frequency-selective block Rayleigh fading
	L=16-path uniform power delay profile
FDE weight	MMSE
Channel estimation & Fast AGC	Ideal

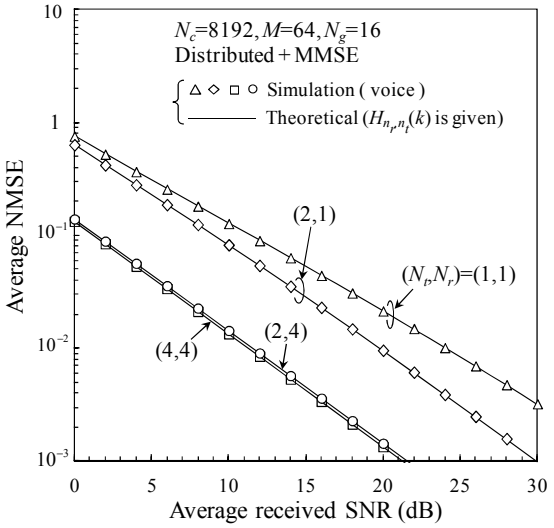

Fig. 4. NMSE performance of analog SC-FDE using joint STTD and receive antenna diversity.

V. Conclusion

In this paper, we proposed analog SC-FDE using joint STTD and receive antenna diversity in order to achieve further performance improvement of analog SC-FDE. We showed that the STBC encoding and decoding technique can be applied not only to digital signal transmission but also to the analog signal transmission. A theoretical analysis of the NMSE performance was presented to evaluate the transmission performance of the proposed scheme and was confirmed by computer simulation. The numerical evaluation and computer simulation showed that joint STTD and receive antenna diversity can significantly improve the performance of recently proposed analog SC-FDE owing to the increase of antenna diversity gain. In this paper, the ideal channel estimation was assumed. Channel estimation for the analog SC-FDE using joint STTD and receive antenna diversity is left as an interesting future study.

References

[1] Y. Park and F. Adachi, *Enhanced radio access technologies for next generation mobile communication*, Springer, 2007.

[2] A. Goldsmith, *Wireless communications*, Cambridge University Press, 2005.

[3] T.H. Vo, S. Kumagai, T. Obara, and F. Adachi, "Analog single-carrier transmission with frequency-domain equalization," Proc. The 19th Asia-Pacific Conference on Communication (APCC2013), pp. 698-702, Aug. 2013.

[4] F. Adachi, H. Tomeba, and K. Takeda, "Introduction of frequency-domain signal processing to broadband single-carrier transmission in a wireless channel," IEICE Trans. Commun., vol. E92-B, no. 9, pp. 2789-2808, Sept. 2009.

[5] R. T. Derryberry, S. D. Gray, D. M. Lonescu, G. Mandyam, and B. Raghothaman, "Transmit diversity in 3G CDMA systems," IEEE Commun. Mag., vol. 40, no. 4, pp. 68-75, April 2002.

[6] S. M. Alamouti, "A simple transmit diversity technique for wireless communications," IEEE J. Select. Areas. Commun., vol. 16, no. 8, pp. 1451-1458, Oct. 1998.

[7] K. Takeda and F. Adachi, "MMSE frequency-domain equalization combined with space-time transmit diversity and antenna received diversity for DS-CDMA," Proc. IEEE 59th Vehicular Technology Conference (VTC2004-Spring), vol. 1, pp. 464-468, May 2004.

[8] R. Matsukawa, T. Obara, K. Takeda and F. Adachi, "Downlink throughput performance of distributed antenna network using transmit/receive diversity," Proc. IEEE 74th Vehicular Technology Conference (VTC2011-Fall), pp. 1-5, Sept. 2011.

[9] Y. Han, Z. Wang, L. Li, and Y. Zhao, "A fast automatic gain control scheme for IEEE 802.15.4 receiver," Proc. IET 2nd International Conference on Wireless, Mobile and Multimedia Networks (ICWMMN 2008), pp. 12-15, Oct. 2008.

[10] H. G. Myung, J. Lim, and D. J. Goodman, "Single carrier FDMA for uplink wireless transmission," IEEE Vehicular Technol. Mag., vol. 1, no. 3, pp. 30-38, Sept. 2006.

APPENDIX: DERIVATION OF σ^2_{ISI} AND $\sigma^2_{\mathrm{noise}}$.

First, we derive σ^2_{ISI} and $\sigma^2_{\mathrm{noise}}$ in case of N_t=2 before generalizing the result for an arbitrary number of transmit antennas. Without loss of generality, σ^2_{ISI} and $\sigma^2_{\mathrm{noise}}$ is derived for the case of j=0 in Eq. (15). In this case, $\mu_{\mathrm{ISI}}(n)$ and $\mu_{\mathrm{noise}}(n)$ are expressed as

$$\begin{cases} \mu_{\mathrm{ISI}}(n) = \dfrac{\dfrac{1}{M}\displaystyle\sum_{k=0}^{M-1}\sum_{n_r=0}^{N_r-1}\sum_{n_t=0}^{1}\widetilde{H}_{n_r,n_t}(k)\left\{\sum_{\substack{n'=0\\ n'\neq n}}^{M-1} s_0(n')\exp\left(j2\pi k\dfrac{n-n'}{M}\right)\right\}}{\dfrac{1}{M}\displaystyle\sum_{k=0}^{M-1}\sum_{n_r=0}^{N_r-1}\sum_{n_t=0}^{1}\widetilde{H}_{n_r,n_t}(k)} \\ \mu_{\mathrm{noise}}(n) = \dfrac{\dfrac{1}{\sqrt{M}}\displaystyle\sum_{k=0}^{M-1}\sum_{n_r=0}^{N_r-1}\left(W^*_{n_r,0}(k)\Pi_{0,n_r}(k)+W^*_{n_r,1}(k)\Pi^*_{1,n_r}(k)\right)\exp\left(j2\pi n\dfrac{k}{M}\right)}{\sqrt{\dfrac{2P}{N_t}}\dfrac{1}{M}\displaystyle\sum_{k=0}^{M-1}\sum_{n_r=0}^{N_r-1}\sum_{n_t=0}^{1}\widetilde{H}_{n_r,n_t}(k)} \end{cases}. \tag{A.1}$$

From Eq. (A.1), σ^2_{ISI} is derived as

$$\sigma^2_{\mathrm{ISI}} = E[|\,\mathrm{Re}\{\mu_{\mathrm{ISI}}(n)\}\,|^2] = \frac{1}{2}E[|\,\mu_{\mathrm{ISI}}(n)\,|^2]$$

$$= \frac{1}{2}\times\frac{\dfrac{1}{M^2}\displaystyle\sum_{k=0}^{M-1}\sum_{k'=0}^{M-1}\sum_{n_r=0}^{N_r-1}\sum_{n_r'=0}^{N_r-1}\sum_{n_t=0}^{1}\sum_{n_t'=0}^{1}\widetilde{H}_{n_r,n_t}(k)\widetilde{H}^*_{n_r',n_t'}(k')}{\left|\dfrac{1}{M}\displaystyle\sum_{k=0}^{M-1}\sum_{n_r=0}^{N_r-1}\sum_{n_t=0}^{1}\widetilde{H}_{n_r,n_t}(k)\right|^2}$$

$$\times\left\{\sum_{m=0}^{M-1}\sum_{\substack{m'=0\\ m\neq n\ m'\neq n}}^{M-1}E[s_0(m)s_0^*(m')]\exp\left[j2\pi\left(k\frac{n-m}{M}-k'\frac{n-m'}{M}\right)\right]\right\}, \tag{A.2}$$

where n=0~M–1. Assuming that the band-limited signal to be transmitted has a uniform power spectrum density, we have $E[s_0(m)s_0^*(m')]=\delta(m-m')$ and then, Eq. (A.2) is rewritten as

$$\sigma^2_{\mathrm{ISI}} = \frac{1}{2}\times\frac{\dfrac{1}{M^2}\displaystyle\sum_{k=0}^{M-1}\sum_{k'=0}^{M-1}\sum_{n_r=0}^{N_r-1}\sum_{n_r'=0}^{N_r-1}\sum_{n_t=0}^{1}\sum_{n_t'=0}^{1}\widetilde{H}_{n_r,n_t}(k)\widetilde{H}^*_{n_r',n_t'}(k')}{\left|\dfrac{1}{M}\displaystyle\sum_{k=0}^{M-1}\sum_{n_r=0}^{N_r-1}\sum_{n_t=0}^{1}\widetilde{H}_{n_r,n_t}(k)\right|^2} \tag{A.3}$$

$$\times\left\{\sum_{m=0}^{M-1}\exp\left(j2\pi(k-k')\frac{n-m}{M}\right)-1\right\}.$$

Using the relationship

$$\sum_{m=0}^{M-1}\exp\left[j2\pi(k-k')\frac{n-m}{M}\right] = M\delta(k-k'), \tag{A.4}$$

we obtain

$$\sigma^2_{\mathrm{ISI}} = \frac{1}{2}\cdot\frac{\dfrac{1}{M^2}\displaystyle\sum_{k=0}^{M-1}\sum_{k'=0}^{M-1}\sum_{n_r=0}^{N_r-1}\sum_{n_r'=0}^{N_r-1}\sum_{n_t=0}^{1}\sum_{n_t'=0}^{1}\widetilde{H}_{n_r,n_t}(k)\widetilde{H}^*_{n_r',n_t'}(k')\{M\delta(k-k')-1\}}{\left|\dfrac{1}{M}\displaystyle\sum_{k=0}^{M-1}\sum_{n_r=0}^{N_r-1}\sum_{n_t=0}^{1}\widetilde{H}_{n_r,n_t}(k)\right|^2}$$

$$= \frac{1}{2}\cdot\frac{\dfrac{1}{M}\displaystyle\sum_{k=0}^{M-1}\left|\sum_{n_r=0}^{N_r-1}\sum_{n_t=0}^{1}\widetilde{H}_{n_r,n_t}(k)\right|^2-\left|\dfrac{1}{M}\displaystyle\sum_{k=0}^{M-1}\sum_{n_r=0}^{N_r-1}\sum_{n_t=0}^{1}\widetilde{H}_{n_r,n_t}(k)\right|^2}{\left|\dfrac{1}{M}\displaystyle\sum_{k=0}^{M-1}\sum_{n_r=0}^{N_r-1}\sum_{n_t=0}^{1}\widetilde{H}_{n_r,n_t}(k)\right|^2}. \tag{A.5}$$

Next, $\sigma^2_{\mathrm{noise}}$ is derived. From Eq. (A.1), we have

$$\sigma^2_{\mathrm{noise}} = E[|\,\mathrm{Re}\{\mu_{\mathrm{noise}}(n)\}\,|^2] = \frac{1}{2}E[|\,\mu_{\mathrm{noise}}(n)\,|^2]$$

$$= \frac{1}{2}\times\frac{1}{\dfrac{2P}{N_t}\left|\dfrac{1}{M}\displaystyle\sum_{k=0}^{M-1}\sum_{n_r=0}^{N_r-1}\sum_{n_t=0}^{1}\widetilde{H}_{n_r,n_t}(k)\right|^2}$$

$$\times\left\{\frac{1}{M}\sum_{k=0}^{M-1}\sum_{k'=0}^{M-1}\sum_{n_r=0}^{N_r-1}\sum_{n_r'=0}^{N_r-1}\left(W^*_{n_r,0}(k)W_{n_r',0}(k')E\left[\hat{\Pi}_{0,n_r}(k)\hat{\Pi}^*_{0,n_r'}(k')\right]\right.\right.$$

$$+W_{n_r,1}(k)W_{n_r',0}(k')E\left[\hat{\Pi}^*_{1,n_r}(k)\hat{\Pi}^*_{0,n_r'}(k')\right]$$

$$+W^*_{n_r,0}(k)W^*_{n_r',1}(k')E\left[\hat{\Pi}_{0,n_r}(k)\hat{\Pi}_{1,n_r'}(k')\right]$$

$$\left.\left.+W_{n_r,1}(k)W^*_{n_r',1}(k')E\left[\hat{\Pi}^*_{1,n_r}(k)\hat{\Pi}_{1,n_r'}(k')\right]\right)\right\}\times\exp\left(j2\pi n\frac{k-k'}{M}\right). \tag{A.6}$$

Since $\{\hat{\Pi}_{q,n_r}(k);\ k$=0~$M$–1, q=0~Q–1, n_r=0~N_r–1$\}$ are the independent and identically distributed (i.i.d) zero-mean complex-valued Gaussian variables having the variance $2N_0/T_s$, we obtain

$$\sigma^2_{\mathrm{noise}} = \frac{1}{2}\times\frac{N_t\times\dfrac{1}{\Gamma}\times\dfrac{1}{M}\displaystyle\sum_{k=0}^{M-1}\sum_{n_r=0}^{N_r-1}\sum_{n_t=0}^{1}|\,W_{n_r,n_t}(k)\,|^2}{\left|\dfrac{1}{M}\displaystyle\sum_{k=0}^{M-1}\sum_{n_r=0}^{N_r-1}\sum_{n_t=0}^{1}\widetilde{H}_{n_r,n_t}(k)\right|^2}. \tag{A.7}$$

From Eqs. (A.5) and (A.7), the generalization of σ^2_{ISI} and $\sigma^2_{\mathrm{noise}}$ for the arbitrary number of transmit antennas can be written as Eqs. (19) and (20).